HETEROCYCLES, Vol. 95, No. 1, 2017, pp. 353-369. © 2017 The Japan Institute of Heterocyclic Chemistry
Received, 7th August, 2016, Accepted, 3rd October, 2016, Published online, 11th November, 2016
DOI: 10.3987/COM-16-S(S)25

SYNTHESIS AND ELECTROCHEMICAL PROPERTIES OF AZULENE-SUBSTITUTED TETRACYANOBUTADIENE AND DICYANOQUINODIMETHANE CHROMOPHORES CONNECTED WITH NAPHTHALENE CORES

Taku Shoji,[a]* Mitsuhisa Maruyama,[a] Akifumi Maruyama,[a] Daichi Nagai,[a] Miwa Tanaka,[a] Ryuta Sekiguchi,[b] Shunji Ito,[b] and Tetsuo Okujima[c]

[a] Department of Chemistry, Faculty of Science, Shinshu University, Matsumoto, 390-8621, Japan. E-mail: tshoji@shinshu-u.ac.jp

[b] Graduate School of Science and Technology, Hirosaki University, Hirosaki 036-8561, Japan

[c] Department of Chemistry and Biology, Graduate School of Science and Engineering, Ehime University, Matsuyama 790-8577, Japan

Dedicated to Professor Masakatsu Shibasaki on the occasion of his 70th birthday

Abstract – Azulene-substituted tetracyanobutadienes (AzTCBDs) and dicyanoquinodimethanes (AzDCNQs) connected with naphthalene cores were prepared by the reaction of 1-azulenylalkynes with tetracyanoethylene (TCNE) and 7,7,8,8-tetracyanoquinodimethane (TCNQ) in a formal [2 + 2] cycloaddition–retroelectrocyclization. The characteristic intramolecular charge transfer (ICT) characters were investigated by using UV/Vis spectroscopy and theoretical calculation. The redox behaviors of AzTCBDs and AzDCNQs were examined by cyclic voltammetry and differential pulse voltammetry, which revealed their properties of multi-electron transfer depending on the number of AzTCBD and AzDCNQ moieties. Moreover, significant color changes were observed by visible spectroscopy under the electrochemical reduction conditions.

INTRODUCTION

Naphthalene is one of the simple polycyclic aromatic hydrocarbons, and its derivatives have been used as a component of photovoltaic devices,[1] organic field-effect transistors,[2] and nonlinear optics.[3] Moreover, a large number of donor–acceptor systems composed by naphthalene derivatives have been synthesized and

their properties represented by their characteristic optical and redox properties have been extensively studied.[4]

Click-type formal [2 + 2] cycloaddition–retroelectrocyclization (CA−RE) of electron-rich alkynes with tetracyanoethylene (TCNE) and 7,7,8,8-tetracyanoquinodimethane (TCNQ), which gives the corresponding 1,1,4,4-tetracyanobutadienes (TCBDs)[5] and dicyanoquinodimethanes (DCNQs),[6] is one of the efficient procedures for the construction of donor–acceptor chromophores. Diederich *et al*. have extensively explored the fields of these chemistries. One of these studies, they reported that 4,4'-(ethyne-1,2-diyldi-4,1-phenylene)bis(4,5-dihydro-3*H*-dinaphtho[2,1-*c*:1',2'-*e*]azepine) and 4,4'-[1,3-butadiyne-1,4-diylbis(benzene-4,1-diyl)]bis-4,5-dihydro-3*H*-dinaphtho[1,2-*e*:2',1'-*c*]azepine react with TCNE to give the corresponding TCBDs possessing binaphthyl groups (Figure 1).[7] Although these compounds were the first examples of TCBD derivatives having naphthalene moieties, TCBDs directly connected to naphthalene ring have not yet been explored.

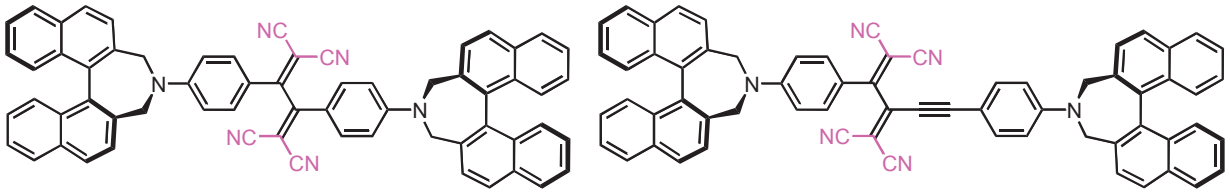

Figure 1. Structure of 3,5-dihydro-4*H*-dinaphtho[2,1-*c*:1',2'-*e*]azepines with a TCBD group

We have also reported the synthesis of azulene-substituted TCBDs (AzTCBDs)[8] and DCNQs (AzDCNQs)[9] connected with various aryl groups, which have been prepared by the [2 + 2] CA–RE reaction of the corresponding ethynylazulene derivatives with TCNE and TCNQ. In these studies, we have revealed that AzTCBDs and AzDCNQs show the significant color changes, which depended on the connected π-electron system, under the electrochemical reduction. Since the optical and electrochemical properties of the AzTCBDs and AzDCNQs are significantly affected by substituted π-electron systems and also the number of the TCBD and DCNQ units in the molecule, AzTCBDs and AzDCNQs with 1- and 2-naphthyl group might be very promising because of the characteristic optical and redox properties of naphthalene as a simple polycyclic aromatic hydrocarbon. Moreover, the intramolecular electronic interaction between the TCBD and DCNQ units should exhibit the characteristics in the multiple AzTCBD and AzDCNQ units in the molecule through the naphthalene core. Therefore, we have examined the systematic investigation of the effect of the naphthalene ring connected to the AzTCBD and AzDCNQ units to provide useful information for the creation of the electronic devices utilizing their redox properties.

Herein, we describe an effect of substituted position of AzTCBDs and AzDCNQs on the naphthalene ring and the number of the TCBD and DCNQ units in the molecule toward optical and electrochemical properties. AzTCBDs and AzDCNQs were prepared by the Pd-catalyzed coupling of 1-ethynylazulene with 1-iodo- or 2-trifluoromethanesulfoxynaphthalene, or a 1-iodoazulene derivative with diethynylnaphthalenes, followed by the [2 + 2] CA–RE reaction of the prepared alkyne precursors with TCNE and TCNQ. The electronic properties of the new AzTCBDs and AzDCNQs with naphthalene core were investigated by absorption spectroscopy and electrochemical analysis. The analyses revealed the significant difference in the properties of the molecules toward the substituted position and the number of AzTCBD and AzDCNQ units on the naphthalene ring.

RESULTS AND DISCUSSION

Synthesis: Preparation of the corresponding 1-azulenylethynylnaphthalene derivatives **3** and **4** was accomplished by a Pd-catalyzed alkynylation of the 1-iodo- or 2-trifluoromethanesulfoxynaphthalenes with 1-ethynylazulene **1**, which was prepared from 2*H*-cyclohepta[*b*]furan-2-one in four-steps procedure.[10] The isopropyl group of **1** serves an essential role to the solubility of the coupling products with a naphthalene core owing to the inhibition of the intermolecular π–π stacking by its steric bulkiness. The cross-coupling reaction of **1** with 1-iodonaphthalene and 2-trifluoromethanesulfoxynaphthalene[11] using [Pd(PPh$_3$)$_4$] as a catalyst and subsequent chromatographic purification on silica gel afforded the desired 1-(1-azulenylethynyl)naphthalene **3** and 2-(1-azulenylethynyl)naphthalene **4** in 84% and 71% yield, respectively.

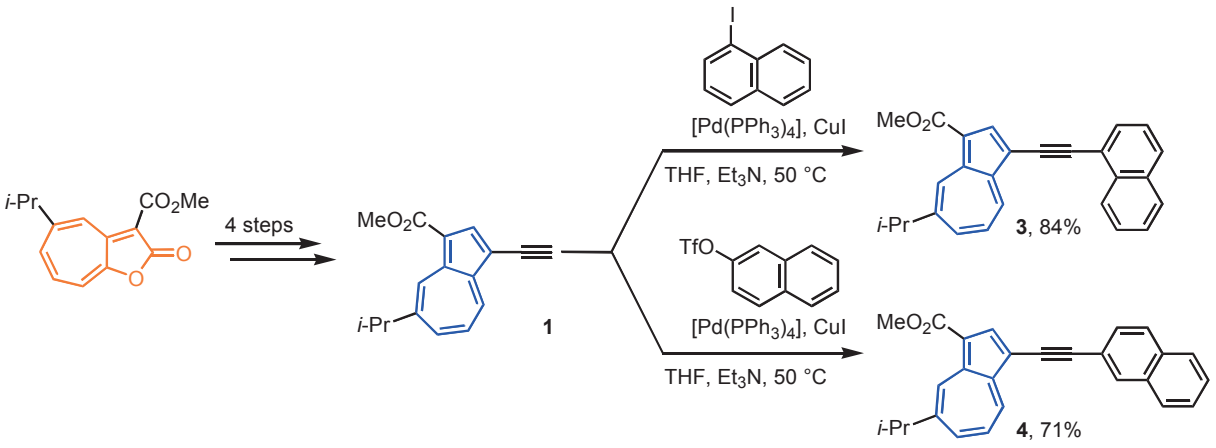

Scheme 1. Synthesis of (1-azulenylethynyl)naphthalenes **3** and **4**

Bis(1-azulenyl)naphthalene derivatives **5**–**8** were also synthesized by Pd-catalyzed alkynylation of **2** with the corresponding diethynylnaphthalenes (Scheme 2). The structure and yield of the products **5**–**8** were

summarized in Figure 2. The cross-coupling reaction of **2**, which was prepared from 2*H*-cyclohepta[*b*]furan-2-one in two-steps,[10] with 1,5-diethynylnaphthalene[12] produced 1,5-bis(1-azulenylethynyl)naphthalene **5** in 82% yield. 1,7-Bis(1-azulenylethynyl)naphthalene **6** was prepared by the reaction of **2** with 1,7-diethynylnaphthalene[13] in 84% yield. A similar Pd-catalyzed reaction of **2** with 2,6-diethynylnaphthalene[14] and 2,7-diethynylnaphthalene[15] yielded 2,6-bis(1-azulenylethynyl)naphthalene **7** and 2,7-bis(1-azulenylethynyl)naphthalene **8** in 94% and 99% yield, respectively.

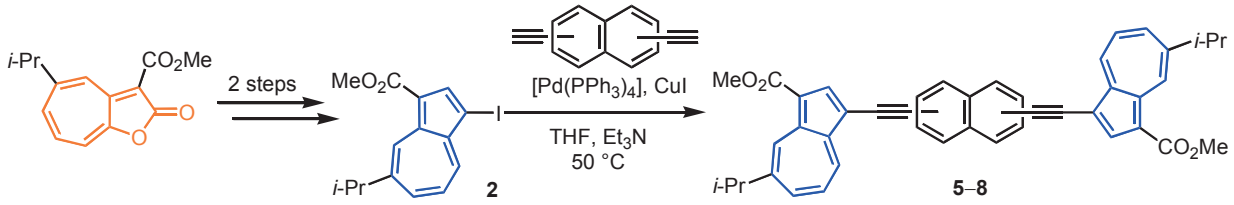

Scheme 2. Synthesis of bis(1-azulenylethynyl)naphthalenes **5**–**8**

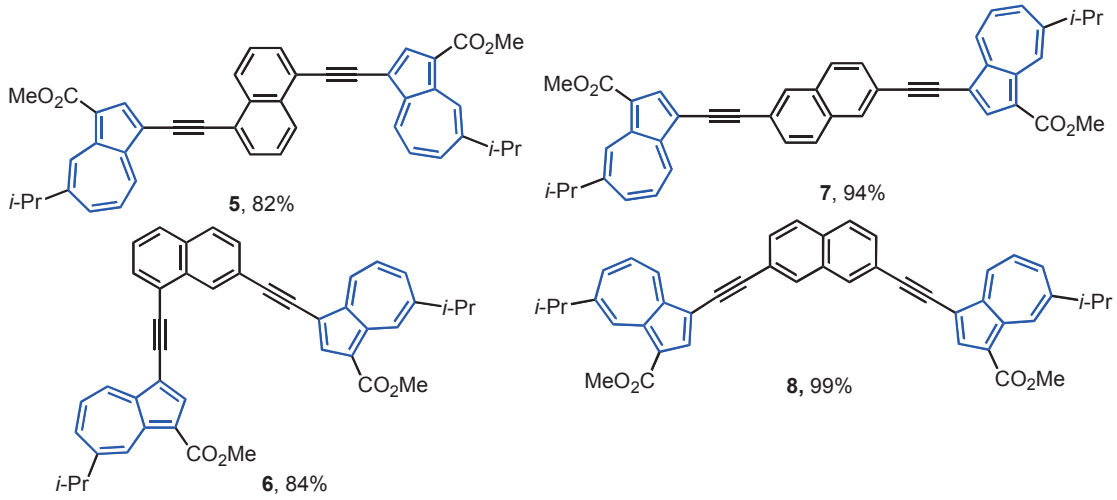

Figure 2. Structure and yield of bis(1-azulenylethynyl)naphthalenes **5**–**8**

To the synthesis of the AzTCBDs **9**–**14** and AzDCNQs **15**–**18** connected with naphthalene core, the [2 + 2] CA–RE sequence was applied to the alkyne derivatives **3**–**8** with TCNE and TCNQ. The reaction of **3** and **4** with TCNE in refluxing ethyl acetate afforded AzTCBDs **9** and **10** in 99% and 90% yield, respectively (Scheme 3).

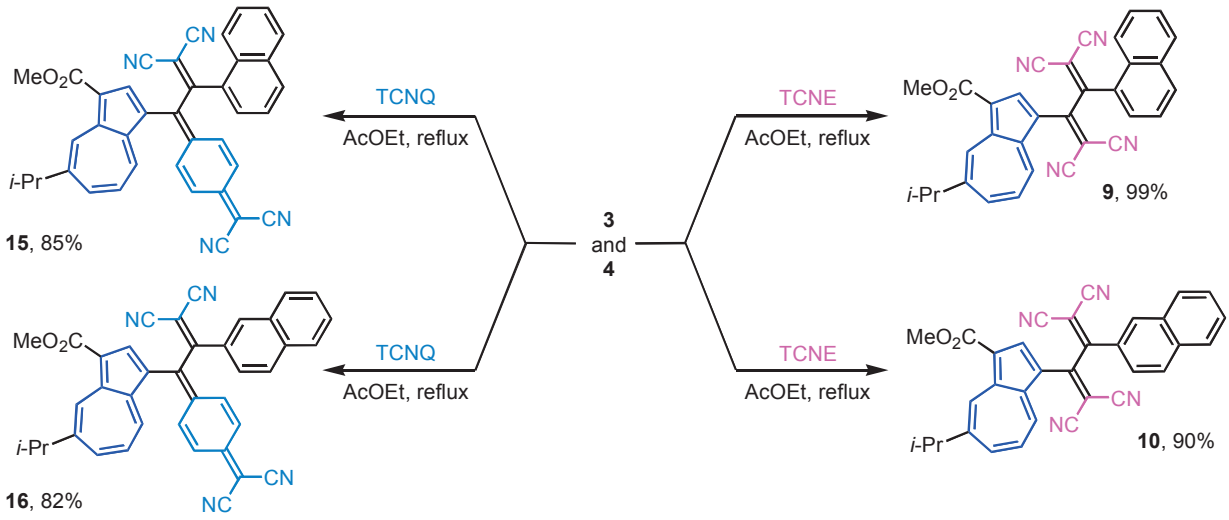

Scheme 3. Reaction of (1-azulenylethynyl)naphthalenes **3** and **4** with TCNE and TCNQ

The naphthalenes bearing two AzTCBD units, bisAzTCBDs **11**−**14**, were also prepared in the same way starting from the corresponding alkynes **5**−**8** (Scheme 4). The structure and yield of the products **11**−**14** are summarized in Figure 2. The double-addition of TCNE with alkyne **5** gave **11** in 91% yield. The TCBD chromophore **12** was also prepared by the CA−RE reaction of **6** with TCNE in 90% yield. BisAzTCBD **13** was obtained in 94% yield by the CA−RE reaction of the alkyne precursor **7** with TCNE. Compound **14** was obtained in 89% by the reaction of TCNE with alkyne **8**. AzTCBDs **9**−**14** were obtained in almost quantitative yield by the formal [2 + 2] CA−RE reaction, although the arrangement of the TCBD units was different on the naphthalene ring. Thus, almost the same yield of the products shows the alkyne arrangement on the naphthalene core does not affect the yield of the products.

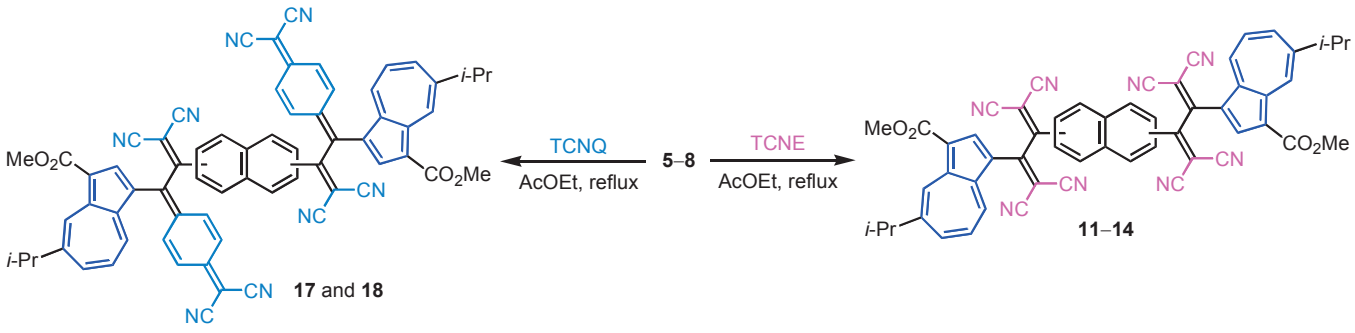

Scheme 4. Reaction of bis(1-azulenylethynyl)naphthalenes **5**−**8** with TCNE and TCNQ

Preparation of AzDCNQs with naphthalene cores was also investigated by the similar manner for the synthesis of the AzTCBDs **9**−**14**. The reaction of alkynes **3**, **4**, **7**, and **8** with TCNQ gave the corresponding AzDCNQs in good yield (Schemes 3 and 4, and Figure 3).[16] However, the [2 + 2] CA–RE

sequence of alkynes **5** and **6** with TCNQ under the similar reaction conditions afforded a complex mixture containing the presumed products. Although the molecular-ion peaks were observed in the crude products by HRMS spectroscopy, formation of the inseparable by-product hampered the isolation of the products.

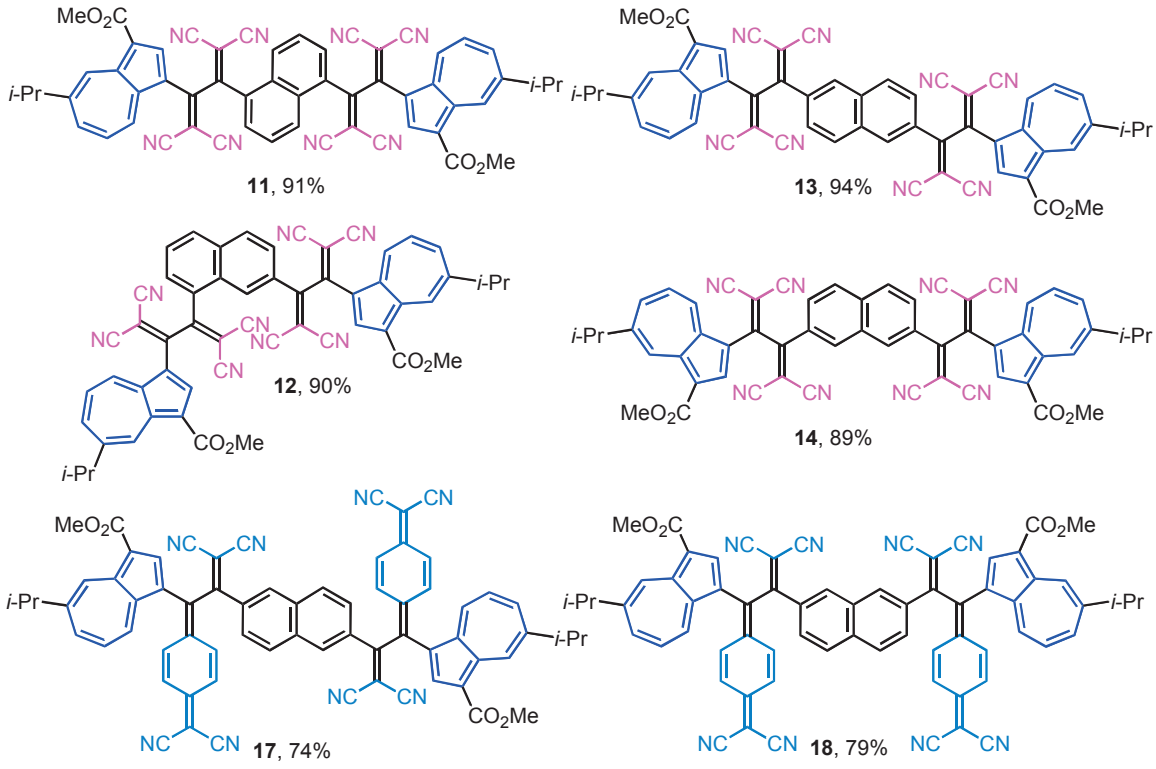

Figure 3. Structure and yield of AzTCBDs **11**−**14**, and 1-AzDCNQs **17** and **18**

Spectroscopic properties: UV/Vis spectra of AzTCBDs **9**−**14** and AzDCNQs **15**−**18** are shown in Supporting Information. The UV/Vis spectra of alkyne derivatives **3**−**8** showed characteristic weak absorptions arising from the azulene system in the visible region. Alkynes **3**−**8** also exhibited relatively strong absorption bands at around 400 nm, which might be explained by the intramolecular charge transfer (ICT) between the azulene and naphthalene moieties through the C≡C triple bond, because these bands could not be observed in that of the 1-ethynylazulene **1**.[10]

UV/Vis spectra of AzTCBDs **9** and **10** showed characteristic broad absorption bands at around 400−700 nm, arising from the presumed ICT absorption between azulene and TCBD units featured by the resonance structure shown in Scheme 5. The end absorption of **9** showed a clear bathochromic shift compared with those of **10** and **19** (Figure 4),[10] although the molar extinction coefficient of the absorption maxima is almost the same value. Usually, the longest wavelength absorption maximum of 1-substituted naphthalene derivatives shows a blue shift compared with that of 2-substituted naphthalenes, due to the

inhibition of co-planarity caused by steric effect between the substituents on 1-position and 8-proton of naphthalene, so called peri-interaction.[17] The hypsochromic shift of **10** might be suggested the less effective conjugation owing to the greater steric interaction among the TCBD moiety and 1,3-protons on the naphthalene ring, rather than the peri-interaction in **9**. Likewise, bisAzTCBDs **11**−**14** also displayed broad absorption bands in visible region, although the extinction coefficients show an increasing trend as the number of AzTCBD units. These effects should be caused by an overlap of ICT arising from the resonance effect among azulene and the two TCBD units.

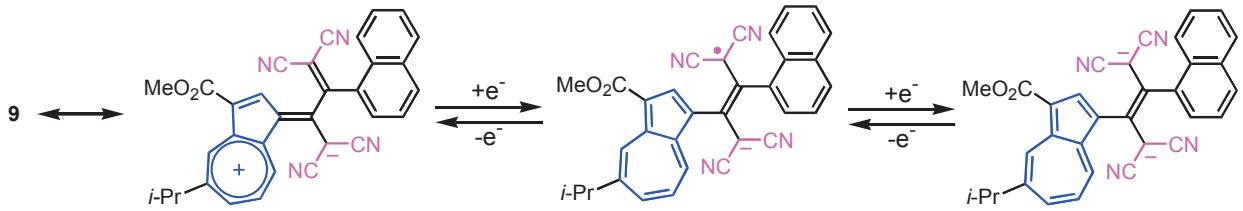

Scheme 5. Plausible resonance structure and redox behavior of AzTCBD **9**

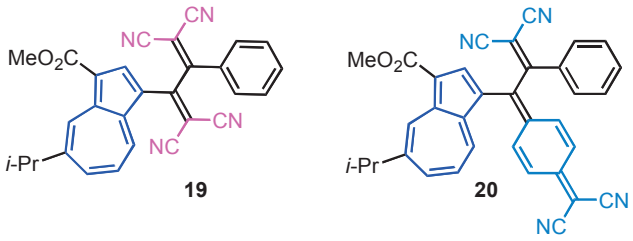

Figure 4. Structure of AzTCBD **19** and AzDCNQ **20** with a phenyl substituent

AzDCNQ chromophores **15** and **16** exhibited a strong absorption band at λ_{max} = 672 nm and λ_{max} = 642 nm in CH_2Cl_2, respectively. Similar to those of AzTCBD derivatives, absorption maxima of **15** showed a clear bathochromic shift compared with those of **16** and **20**[9a] (λ_{max} = 641 nm, Figure 4). The longest wavelength absorption maximum of **16** was in almost the same spectral region with that of bisAzDCNQs **17** (λ_{max} = 650 nm) and **18** (λ_{max} = 644 nm), although the extinction coefficients were in proportion to the number of DCNQ units. These results should be attributed to the effectiveness of π-conjugation between the AzDCNQ unit and 1-naphthyl group, rather than 2-naphthyl and phenyl groups. When the solvent was changed from CH_2Cl_2 to the mixed *n*-hexane/CH_2Cl_2 solvent, the AzDCNQ derivatives **15**−**18** showed negative solvatochromism. Although compound **15** showed the absorption band at 672 nm in CH_2Cl_2, hypsochromic shift of **15** by 51 nm (λmax = 621 nm) was observed in the less polar 90% *n*-hexane/ CH_2Cl_2. These results support the ICT nature of this band (Figures S50, S52, S53 and S55).[18]

To elucidate the nature of the absorption bands of alkynes **3** and **4**, and AzTCBDs **9** and **10**, theoretical calculations were carried out on time-dependent density functional theory (TD-DFT) calculations at the B3LYP/6-31G** level.[19] The frontier Kohn−Sham orbitals of these compounds are shown in the Supporting Information. From the theoretical calculations, the strong absorption bands of **3** (λ_{max} = 403 nm) and **4** (λ_{max} = 402 nm) were considered to be the transition from the HOMO located on the 1-ethynylazulene and naphthalene moieties to the LUMO+1 mainly located on the 1-azulenyl group with the electron-withdrawing methoxycarbonyl substituent. The calculations also revealed the small contribution of HOMO−2 → LUMO in the azulene part in this band (Table 1). Thus, the absorption bands of **3** and **4** at around 400 nm could be assigned to the ICT from the naphthalene-ring to 1-azulenyl group through the connected alkyne moiety. The weak absorption bands of **3** (λ_{max} = 573 nm) and **4** (λ_{max} = 572 nm) in the longest wavelength region were confirmed to arise from the overlap of the π−π* transitions (HOMO → LUMO) of the substituted azulene rings themselves.

Table 1. Electronic transitions for alkynes **3** and **4**, AzTCBDs **9** and **10**, and AzDCNQs **15** and **16** derived from the computed values based on B3LYP/6-31G** method and experimental values

Sample	Experimental	Computed Value	
	λ_{max} (log ε)	λ_{max} (strength)	Composition of band[a] (amplitude)
3	403 (4.21)	406 (0.3804)	H−2 → L (0.2234)
			H → L+1 (0.9115)
	573 (2.86)	576 (0.0072)	H → L (0.9674)
4	402 (4.19)	400 (0.4746)	H−2 → L (0.2570)
			H → L+1 (0.9041)
	572 (2.84)	573 (0.0077)	H → L (0.9674)
9	389 (4.07)	373 (0.0230)	H−1 → L+1 (0.9887)
		404 (0.1698)	H → L+2 (0.9223)
		451 (0.0331)	H−1 → L (0.9807)
	466 (3.95)	475 (0.1150)	H → L (0.5464)
			H → L+1 (0.7649)
	550 sh (3.85)	488 (0.0843)	H → L (0.7862)
10	398 (4.23)	386 (0.3995)	H−1 → L+1 (0.3239)
			H → L+1 (0.8747)
		390 (0.0753)	H−1 → L+2 (0.9446)
		406 (0.0570)	H−1 → L (0.8953)
		410 (0.0071)	H−1 → L (0.3851)
			H−1 → L+1 (0.8631)
	459 (4.15)	453 (0.0319)	H → L (0.3558)
	530 sh (3.98)		H → L+2 (0.9230)

[a] H = HOMO, L = LUMO

On the basis of both experimental and theoretical UV/Vis spectra, the broad absorption bands of **9** and **10** in the visible region could be assigned to the transition originating from the HOMO located on azulene ring and the HOMO–1 located at the naphthalene ring to the LUMO, LUMO+1 and LUMO+2 spread in azulene, naphthalene and TCBD moieties. Thus, the broad absorption bands for **9** could be assigned to overlapping of CT absorptions from the both 1-azulenyl and naphthyl moieties to the TCBD unit. The theoretical calculation also revealed the lower HOMO-LUMO gap of **9** (7.64 eV) compared to that of **10** (8.06 eV). Thus, bathochromic shift of end absorption of **9** compared to that of **10** should be ascribed to the effectiveness of extension of the π-electron system by 1-naphthyl group in **9** rather than that by 2-naphthyl group in **10**.

Electrochemistry: To clarify the effect on the electrochemical properties of the substitution position on the naphthalene ring in AzTCBD and AzDCNQ derivatives, the redox behavior of AzTCBDs **9**−**14** and AzDCNQs **15**−**18** was examined by CV and DPV.[20] The redox potentials (in volts vs. $Ag/AgNO_3$) of these compounds are summarized in Table 2.

As shown in Table 2, the reduction potentials were significantly affected by the substituted position of AzTCBD and AzDCNQ on naphthalene ring. Multi-stage reduction of AzTCBDs **9**−**14** and AzDCNQs **15**−**18** should be attributed to the two-step reduction to dianionic species in each TCBD and DCNQ unit as represented in Scheme 5. Electrochemical reduction of **9** showed a two-step reduction wave with the half-wave potentials of −0.54 V and −1.04 V upon CV, which can be attributed to the formation of a radical anionic and a dianionic species, respectively (Scheme 5). A two-stage wave was also observed by CV in **10** (−0.62 V and −1.02 V) to form a dianionic species. The first reduction potential of **9** (−0.54 V) showed a lower potential than that of **10** (−0.62 V) and **19** (−0.61 V) probably due to the effective conjugation between AzTCBD unit and naphthalene ring that lowed the LUMO level, as predicted by theoretical calculation and UV/Vis spectra. BisAzTCBDs **11**−**14** exhibited the less negative first reduction potential compared with that of **9** and **10**. Although the bisAzTCBDs **11**, **13** and **14** have a symmetrical structure, two TCBD units showed a stepwise reduction by CV, which should be corresponded to the generation of multivalent anion. These results indicate the existence of redox interaction between the two AzTCBD moieties through the central naphthalene spacer.

The first reduction potential of **12** (−0.45 V), which possesses TCBD units on both α- and β-position of naphthalene ring, was the same value with that of **11** (−0.45 V). The value suggests the TCBD unit of **12** on the α-position preferentially reduced by electrochemical reaction, rather than that on the β-position. The electrochemical reduction of **13** displayed a four-step reduction wave by CV due to the formation up to a tetraanionic species. BisAzTCBD **14** also exhibited a four-step reduction wave. This phenomenon

might be ascribed to the intramolecular redox interaction between the two AzTCBD units through the cross-conjugation of the naphthalene spacer.[21]

Table 2. Redox potentials[a,b] of AzTCBDs **9**−**14** and AzDCNQs **15**−**18** with a naphthalene ring and AzTCBD **19** and AzDCNQ **20** with a phenyl substituent for comparison

Sample	Method	E_1^{Red} [V]	E_2^{Red} [V]	E_3^{Red} [V]	E_4^{Red} [V]
9	CV	−0.54	−1.04		
	(DPV)	(−0.52)	(−1.02)	(−2.00)	
10	CV	−0.62	−1.02		
	(DPV)	(−0.60)	(−1.00)	(−1.96)	
11	CV	−0.45	−0.59	−1.07	
	(DPV)	(−0.43)	(−0.57)	(−1.05)	
12	CV	−0.45	−0.63	−1.10	
	(DPV)	(−0.43)	(−0.63)	(−1.08)	(−1.21)
13	CV	−0.52	−0.65	−1.02	−1.10
	(DPV)	(−0.50)	(−0.63)	(−1.00)	(−1.08)
14	CV	−0.54	−0.63	−1.02	−1.10
	(DPV)	(−0.52)	(−0.61)	(−1.00)	(−1.08)
15	CV	−0.39	−0.59		
	(DPV)	(−0.37)	(−0.57)	(−1.96)	
16	CV	−0.46	−0.62		
	(DPV)	(−0.44)	(−0.60)	(−1.98)	
17	CV	−0.45	−0.61		
	(DPV)	(−0.43)	(−0.59)	(−1.98)	
18	CV	−0.46	−0.63		
	(DPV)	(−0.44)	(−0.61)	(−1.99)	
19[10]	CV	−0.61	−1.03		
	(DPV)	(−0.59)	(−1.01)	(−1.95)	
20[9a]	CV	−0.43	−0.59		
	(DPV)	(−0.41)	(−0.58)	(−0.90)	(−1.93)

[a] V vs. $Ag/AgNO_3$, 1 mM in benzonitrile containing Et_4NClO_4 (0.1 M), Pt electrode (internal diameter: 1.6 mm), scan rate = 100 mVs^{-1}, and internal reference (Fc/Fc^+ = +0.15 V). [b] Half-wave potentials E^{Red} = (E_{pc} + E_{pa})/2 on CV, E_{pc} and E_{pa} correspond to the cathodic and anodic peak potentials, respectively.

Electrochemical reduction of AzDCNQs **15**−**18** also showed a two-stage reduction wave on CV, which could be attributed to the formation of anionic species. The AzDCNQs **15**−**18** exhibited more negative reduction potentials compared with those of the corresponding AzTCBDs **9**−**14**. These results are ascribed to the higher electron-accepting nature of the DCNQ moieties than that of the corresponding TCBD derivatives. Similar to the results on the AzTCBDs, the AzDCNQ **15** showed reduction potentials nobler than those of AzDCNQs **16** and **20**. These results also support the assumption of the effectiveness of π-conjugation between the AzDCNQ unit and 1-naphthyl group, rather than 2-naphthyl and phenyl groups. Electrochemical reduction of bisAzDCNQs **17** and **18** displayed only two-waves on CV, although there are two AzDCNQ units in each molecule. These results indicate that the two DCNQ units in bisAzDCNQs **17** and **18** are reduced simultaneously in each step under the electrochemical reduction conditions. Moreover, reduction potentials of bisAzDCNQs **17** and **18** are consistent with that of AzDCNQ **16** with 2-naphthyl group. Therefore, the redox interaction among the two AzDCNQ moieties through the naphthalene ring is almost negligible from the view point of electrochemical reduction.

In summary, spectral and electrochemical features of AzTCBDs and AzDCNQs were directly affected by substituted position of AzTCBD and AzDCNQ units on naphthalene ring. The 1-naphthyl group is effectively extended the π-conjugation, rather than 2-naphthyl and phenyl groups. Moreover, electronic interaction among the two AzTCBD units on naphthalene ring was revealed by their voltammetric analyses, although the redox reaction of bisAzDCNQs **17** and **18** are caused independently by each AzDCNQ unit.

Previously, Hünig *et al*. proposed a violene–cyanine hybrid for the design of a stabilized organic electrochromic systems.[22] We have identified some new hybrid structures of violenes and cyanines during the study on the synthesis and redox behavior of TCBDs and DCNQs connected with various π-electron systems.[8,23,24] Similar to these TCBDs and DCNQs derivatives, new AzTCBDs **9**−**14** and AzDCNQs **15**−**18** might become the redox systems for the extensions of the hybrid structures of violenes and cyanines. Thus, the visible spectra of AzTCBDs **9**−**14** and AzDCNQs **15**−**18** were monitored to clarify the color changes observed during the electrochemical reactions.[24]

When the spectral changes of **9** were monitored under the electrochemical reduction conditions at −0.80 V, the absorption band in the visible region gradually increased with the development of new absorption bands at around λ_{max} = 550−900 nm, along with isosbestic point at λ_{max} = 530 nm. The spectral changes should be attributable to the formation of an anionic species formed by the electrochemical reduction of **9**. Reverse oxidation of the reduced species regenerated the original spectrum of **9** (Figure 5).

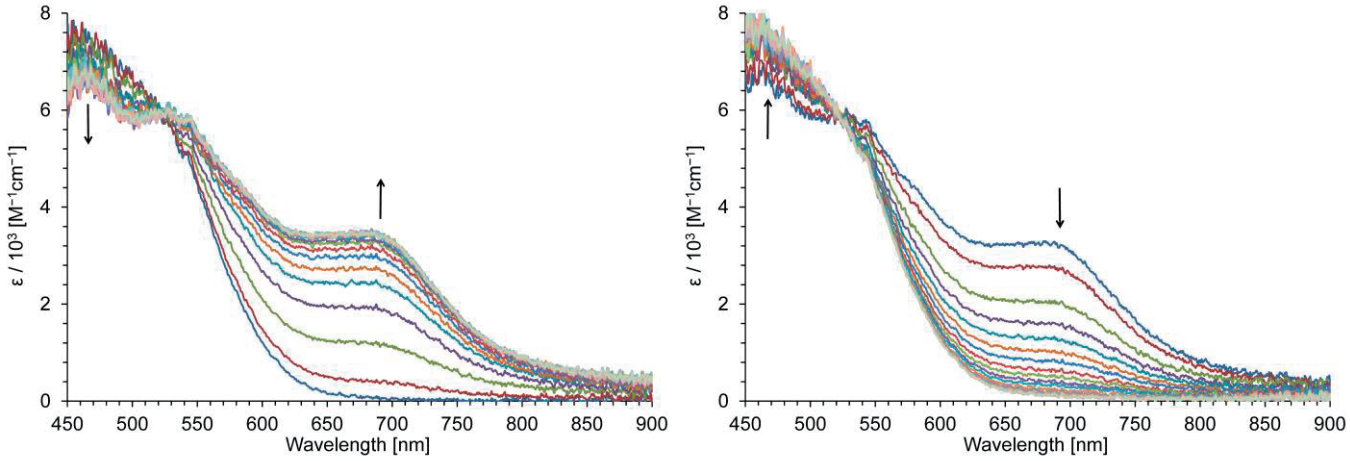

Figure 5. Continuous change in the visible spectrum of **9** under constant voltage electrochemical reduction (−0.80 V, top) and reverse electrochemical oxidation (−0.10 V, bottom) in benzonitrile containing Et_4NClO_4 (0.10 M) at 30 sec intervals

Electrochemical reduction of AzTCBD **10** at −0.85 V showed the development of an absorption band at around 700 nm along with an isosbestic point at λ_{max} = 525 nm. Reverse oxidation of the reduced species regenerated the original spectrum of **10** (Figure S41). Similar with those of **9** and **10**, the reversible spectral changes were observed in electrochemical redox reactions of bisAzTCBDs **11**−**14** (Figure S43, S45, S47 and S49). The reversibility for the electrochromisms of AzTCBDs **9**−**14** is referred to the high stability of the anionic species produced by the electrochemical reduction.

When the spectral changes of AzDCNQ **15** were monitored during the electrochemical reduction at −1.00 V, only decrease in the intensity of the absorption band in the visible region was observed. The color change is attributable to the formation of anionic species formed by the reduction of **15**. Reverse oxidation of the reduced species regenerated the original spectrum of **15** (Figure S51). As suggested by the results on CV, the reversible spectral change noted for **15** should be ascribed by the two electron reduction of the AzDCNQ unit to form dianionic species. The longest absorption band of AzDCNQ **16** gradually decreased along with generation of the new absorption at λ_{max} = 610 nm was developed during the electrochemical reduction at −0.52 V, and further reduction at −1.00 V decreased the new absorption band. Reversible oxidation of reduced species gradually regenerated the spectra of the corresponding original compound (Figure 6).

Similar with those of **15** and **16**, the absorption bands of **17** in the visible region gradually disappeared along with an increase in the new absorption bands at the infrared region during the electrochemical reduction at −1.00 V. The reverse oxidation partially regenerated the parent spectrum of **17** (Figure S54). When visible spectra of **18** were measured under the electrochemical reduction conditions, absorption bands of **18** in the visible region gradually decreased coincident with a development of new absorption

bands in the infrared region. Reverse oxidation recovered the original absorption of **18**, but incompletely (Figure S56). Usually, the most of the electrochromic compounds change from a colorless state to a colored state upon electrochemical reaction conditions.[26] In 2013, Abe and co-workers reported the negative photochromic system composed by imidazole derivative, in which the stable colored species converts to the metastable colorless species by the visible light irradiation.[27] Similar with negative photochromic system, AzDCNQs **15**−**18** could be behaved as a negative electrochromic system, since the deep colored species turned to colorless species by the electrochemical reaction.

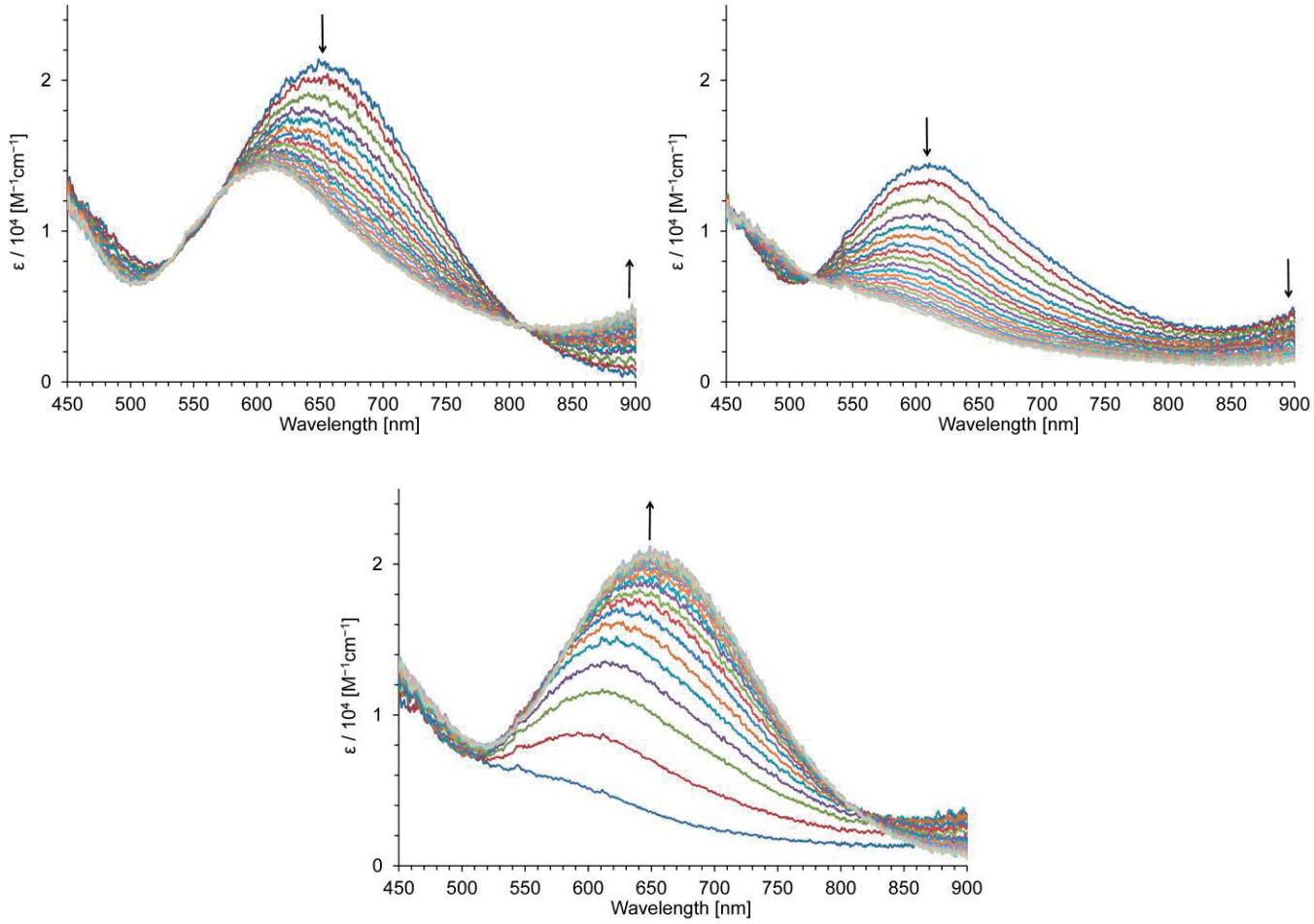

Figure 6. Continuous change in the visible spectrum of **16** under constant voltage electrochemical reduction (−0.52 V, top left), further electrochemical reduction (−1.00, top right) and reverse electrochemical oxidation (−0.10 V, bottom) in benzonitrile containing Et_4NClO_4 (0.10 M) at 30 sec intervals

CONCLUSION

A series of 1-ethynylazulene derivatives **3**−**8**, which were prepared from 2*H*-cyclohepta[*b*]furan-2-one as starting material, with a naphthalene core were prepared by palladium-catalyzed Sonogashira−Hagihara reaction. The AzTCBDs **9**−**14** and AzDCNQs **15**−**18** connected with a naphthalene ring were synthesized

in a one-step procedure consisting of formal [2 + 2] cycloaddition reaction of alkynes **3**−**8** with TCNE and TCNQ, followed by retroelectrocyclization of the initially formed cyclobutene derivatives. The ICT absorption bands were found in UV/Vis spectra of the AzTCBDs **9**−**14** and AzDCNQs **15**−**18**. Analyses by CV and DPV showed that the AzTCBDs **9**−**14** and AzDCNQs **15**−**18** exhibited a reversible multi-stage reduction wave, due to the two-step reduction properties of each TCBD and DCNQ unit. Moreover, reversible color changes of the AzTCBDs **9**−**14** and AzDCNQs **15**−**18** were observed during the redox conditions. AzTCBDs **9**−**14** exhibited spectral changes, in which new absorption bands were appeared in the longer wavelength region, attributable to the generation of anionic species during the electrochemical reaction. Whereas, AzDCNQs **15**−**18** showed unusually a negative electrochromism, in which the colored species changed to colorless ones by the electrochemical reduction.

To evaluate the scope of the class of molecules investigated in this research, the preparation of novel TCBD and AzDCNQ chromophores connected with various π-electron cores is in progress in our laboratory.

EXPERIMENTAL

Melting points were determined with a Yanagimoto MPS3 micro melting apparatus. Mass spectra were obtained with a Bruker APEX II instrument. IR and UV/Vis spectra were measured with JASCO FT/IR-4100 and Shimadzu UV-2550 spectrophotometers. ^{1}H and ^{13}C NMR spectra were recorded with a JEOL ECA500 spectrometer at 500 MHz and 125 MHz, respectively. The voltammetry measurements were carried out in benzonitrile containing Et_4NClO_4 (0.1 M) as a supporting electrolyte by utilizing Pt working and auxiliary electrodes and a reference electrode formed from $Ag/AgNO_3$ (0.01 M) in acetonitrile containing *n*-Bu_4NClO_4 (0.1 M) at a scan rate of 100 mVs^{-1}. The internal reference Fc/Fc^{+} discharges at +0.15 V under these conditions. Experimental detail and chart of ^{1}H and ^{13}C NMR spectra of reported compounds are summarized in Supporting Information.

ACKNOWLEDGEMENTS

This work was supported by JSPS KAKENHI Grant Number JP25810019 and also by a research grant from the Faculty of Science, Shinshu University.

REFERENCES AND NOTES

1. M. Nakano, H. Mori, S. Shinamura, and K. Takimiya, *Chem. Mater.*, 2012, **24**, 190.
2. (a) S. Shinamura, I. Osaka, E. Miyazaki, A. Nakao, M. Yamagishi, J. Takeya, and K. Takimiya, *J. Am. Chem. Soc.*, 2011, **133**, 5024; (b) C. Mitsui, J. Soeda, K. Miwa, H. Tsuji, J. Takeya, and E. Nakamura, *J. Am. Chem. Soc.*, 2012, **134**, 5448.

3. M. Juríček, P. Kasák, M. Stach, and M. Putala, *Tetrahedron Lett.*, 2007, **48**, 8869.
4. (a) V. A. Ozeryanskii, A. F. Pozharskii, A. K. Artaryan, N. V. Vistorobskii, and Z. A. Starikova, *Eur. J. Org. Chem.*, 2009, 1241; (b) Y. Kim, J. Hong, J. H. Oh, and C. Yang, *Chem. Mater.*, 2013, **25**, 3251; (c) G. Kim, S.-J. Kang, G. K. Dutta, Y.-K. Han, T. J. Shin, Y.-Y. Noh, and C. Yang, *J. Am. Chem. Soc.*, 2014, **136**, 9477; (d) Y. Jiang, Y. Gao, H. Tian, J. Ding, D. Yan, Y. Geng, and F. Wang, *Macromolecules*, 2016, **49**, 2135.
5. (a) T. Michinobu, I. Boudon, J.-P. Gisselbrecht, P. Seiler, B. Frank, N. N. P. Moonen, M. Gross, and F. Diederich, *Chem. Eur. J.*, 2006, **12**, 1889; (b) F. Tancini, F. Monti, K. Howes, A. Belbakra, A. Listorti, W. B. Schweizer, P. Reutenauer, J.-L. Alonso-Gómez, C. Chiorboli, L. M. Urner, J.-P. Gisselbrecht, C. Boudon, N. Armaroli, and F. Diederich, *Chem. Eur. J.*, 2014, **20**, 202; (c) G. Jayamurugan, A. D. Finke, J.-P. Gisselbrecht, C. Boudon, W. B. Schweizer, and F. Diederich, *J. Org. Chem.*, 2014, **79**, 426.
6. (a) M. Kivala, C. Boudon, J.-P. Gisselbrecht, P. Seiler, M. Gross, and F. Diederich, *Chem. Commun.*, 2007, 4731; (b) M. Kivala, C. Boudon, J.-P. Gisselbrecht, B. Enko, P. Seiler, I. B. Müller, N. Langer, P. D. Jarowski, G. Gescheidt, and F. Diederich, *Chem. Eur. J.*, 2009, **15**, 4111; (c) S.-i. Kato, M. Kivala, W. B. Schweizer, C. Boudon, J.-P. Gisselbrecht, and F. Diederich, *Chem. Eur. J.*, 2009, **15**, 8687.
7. B. B. Frank, B. C. Blanco, S. Jakob, F. Ferroni, S. Pieraccini, A. Ferrarini, C. Boudon, J.-P. Gisselbrecht, P. Seiler, G. P. Spada, and F. Diederich, *Chem. Eur. J.*, 2009, **15**, 9005.
8. (a) T. Shoji, M. Maruyama, S. Ito, and N. Morita, *Bull. Chem. Soc. Jpn.*, 2012, **85**, 761; (b) T. Shoji, S. Ito, T. Okujima, and N. Morita, *Org. Biomol. Chem.*, 2012, **10**, 8308; (c) T. Shoji, M. Maruyama, A. Maruyama, S. Ito, T. Okujima, and K. Toyota, *Chem. Eur. J.*, 2014, **20**, 11903; (d) T. Shoji, A. Maruyama, E. Shimomura, D. Nagai, S. Ito, T. Okujima, and K. Toyota, *Eur. J. Org. Chem.*, 2015, 1979; (e) T. Shoji, A. Maruyama, M. Tanaka, D. Nagai, E. Shimomura, K. Fujimori, S. Ito, T. Okujima, K. Toyota, and M. Yasunami, *ChemistrySelect*, 2016, **1**, 49; (f) S. Ito and N. Morita, *Eur. J. Org. Chem.*, 2009, 4567; (g) S. Ito, T. Shoji, and N. Morita, *Synlett*, 2011, 2279.
9. (a) T. Shoji, S. Ito, K. Toyota, T. Iwamoto, M. Yasunami, and N. Morita, *Eur. J. Org. Chem.*, 2009, 4316; (b) T. Shoji, E. Shimomura, M. Maruyama, A. Maruyama, S. Ito, T. Okujima, K. Toyota, and N. Morita, *Eur. J. Org. Chem*., 2013, 7785; (c) T. Shoji, M. Maruyama, E. Shimomura, A. Maruyama, S. Ito, T. Okujima, K. Toyota, and N. Morita, *J. Org. Chem.*, 2013, **78**, 12513.
10. T. Shoji, S. Ito, K. Toyota, M. Yasunami, and N. Morita, *Chem. Eur. J.*, 2008, **14**, 8398.
11. M. A. Brimble and M. Y. H. Lai, *Org. Biomol. Chem.*, 2003, **1**, 2084.
12. S. H. Lim and S. M. Cohen, *Inorg. Chem.*, 2013, **52**, 7862.
13. R. F. C. Brown, F. Eastwood, and N. R. Wong, *Tetrahedron Lett.*, 1993, **34**, 1223.

14. A. Zukal, E. Slováková, H. Balcar, and J. Sedláček, *Macromol. Chem. Phys.*, 2013, **214**, 2016.
15. T. X. Neenan and G. M. Whitesides, *J. Org. Chem.*, 1988, **53**, 2489.
16. In the case of **16**, inseparable by-product hampered the complete purification of the product.
17. V. Balasubramaniyan, *Chem. Rev.*, 1966, **66**, 567.
18. (a) P. Suppan and N. Ghoneim, *Solvatochromism*, Royal Society of Chemistry, Cambridge, UK, 1997; (b) P. Suppan, *J. Photochem. Photobiol. A: Chem.*, 1990, **50**, 293; (c) C. Reichardt, *Solvent and Solvent Effects in Organic Chemistry*, Wiley-VCH, New York, 2004.
19. The B3LYP/6-31G** time-dependent density functional calculations were performed with Spartan'10, Wavefunction, Irvine, CA. Although the theoretical calculation of AzDCNQ **15** and **16** was also examined, molecular size and conformational flexibility of these compounds hampered the computational study.
20. The voltammetry measurements were performed with a BAS 100B/W electrochemical workstation equipped with a standard three electrode configuration and all measurements were carried out under an argon atmosphere. Tetraethylammonium perchlorate (0.10 M) in benzonitrile was used as a supporting electrolyte, with a platinum wire auxiliary and disk working electrodes. Reference electrode was formed from $Ag/AgNO_3$ (0.01 M) in acetonitrile containing tetrabutylammonium perchlorate (0.10 M). The half-wave potential of the ferrocene/ferrocenium ion couple (Fc/Fc^+) under these conditions using this reference electrode was observed at +0.15 V on CV. Accuracy of the reference electrode was confirmed by CV measurements of the couple in each sample as an internal ferrocene standard.
21. Redox interaction of AzTCBDs by the cross-conjugation through the 1,3,5-benzenetriyl spacer was previously reported; See reference 10.
22. (a) S. Hünig, M. Kemmer, H. Wenner, I. F. Perepichka, P. Bäuerle, A. Emge, and G. Gescheidt, *Chem. Eur. J.*, 1999, **5**, 1969; (b) S. Hünig, M. Kemmer, H. Wenner, F. Barbosa, G. Gescheidt, I. F. Perepichka, P. Bäuerle, A. Emge, and K. Peters, *Chem. Eur. J.*, 2000, **6**, 2618; (c) S. Hünig, I. F. Perepichka, M. Kemmer, H. Wenner, P. Bäuerle, and A. Emge, *Tetrahedron*, 2000, **56**, 4203; (d) S. Hünig, C. A. Briehn, P. Bäuerle, and A. Emge, *Chem. Eur. J.*, 2001, **7**, 2745; (e) S. Hünig, A. Langels, M. Schmittel, H. Wenner, I. F. Perepichka, and K. Peters, *Eur. J. Org. Chem*., 2001, 1393.
23. (a) T. Shoji, S. Ito, T. Okujima, and N. Morita, *Eur. J. Org. Chem.*, 2011, 5134; (b) T. Shoji, S. Ito, T. Okujima, and N. Morita, *Chem. Eur. J.*, 2013, **19**, 5721; (c) T. Shoji, A. Maruyama, C. Yaku, N. Kamata, S. Ito, T. Okujima, and K. Toyota, *Chem. Eur. J.*, 2015, **21**, 402; (d) T. Shoji, N. Kamata, A. Maruyama, S. Ito, and T. Okujima, *Bull. Chem. Soc. Jpn.*, 2015, **88**, 1338.
24. (a) T. Shoji, J. Higashi, S. Ito, T. Okujima, M. Yasunami, and N. Morita, *Chem. Eur. J.*, 2011, **17**, 5116; (b) T. Shoji, J. Higashi, S. Ito, T. Okujima, M. Yasunami, and N. Morita, *Org. Biomol. Chem*.,

2012, **10**, 2431.

25. Constant-voltage oxidation and reduction was applied to the solutions with a platinum mesh as the working electrode and a wire counter electrode in an electrolytic cell of 1 mm thickness. Visible spectra were measured in degassed benzonitrile containing Et_4NClO_4 (0.1 M) as a supporting electrolyte at room temperature under the electrochemical reaction conditions.
26. P. M. S. Monk, R. J. Mortimer, and D. R. Rosseinsky, *Electrochromism and Electrochromic Devices*, Cambridge University Press, Cambridge, 2007.
27. S. Hatano, T. Horino, A. Tokita, T. Oshima, and J. Abe, *J. Am. Chem. Soc.*, 2013, **135**, 3164.